Journal of Computational Physics 230 (2011) 920–936

Contents lists available at ScienceDirect

Journal of Computational Physics

journal homepage: www.elsevier.com/locate/jcp

A level set approach for dilute non-collisional fluid-particle flows

Hailiang Liu [a,*], Zhongming Wang [b], Rodney O. Fox [c]

[a] Mathematics Department, Iowa State University, Ames, IA 50011, United States
[b] Department of Mathematics, UCSD, La Jolla, CA 92093-0112, United States
[c] Department of Chemical and Biological Engineering, Iowa State University, Ames, IA 50011, United States

ARTICLE INFO

Article history:
Received 2 December 2009
Received in revised form 23 August 2010
Accepted 24 August 2010
Available online 20 November 2010

Keywords:
Level set method
Kinetic equations
Fluid particle fluids

ABSTRACT

Gas-particle and other dispersed-phase flows can be described by a kinetic equation containing terms for spatial transport, acceleration, and particle processes (such as evaporation or collisions). However, computing the dispersed velocity is a challenging task due to the large number of independent variables. A level set approach for computing dilute non-collisional fluid-particle flows is presented. We will consider the sprays governed by the Williams kinetic equation subject to initial distributions away from equilibrium of the form $\sum_{i=1}^{N}\rho_i(x)\delta(\xi-u_i(x))$. The dispersed velocity is described as the zero level set of a smooth function, which satisfies a transport equation. This together with the density weight recovers the particle distribution at any time. Moments of any desired order can be evaluated by a quadrature formula involving the level set function and the density weight. It is shown that the method can successfully handle highly non-equilibrium flows (e.g. impinging particle jets, jet crossing, particle rebound off walls, finite Stokes number flows).

1. Introduction

In this article we develop a level set approach for simulation of dilute non-collisional fluid-particle flows. We are interested in non-equilibrium flows wherein the velocity density function is far from Maxwellian. For example, dilute systems often exhibit non-equilibrium behavior because particle collisions are too weak to overcome kinetic effects. In many cases the velocity density function can be non-unimodal, implying that there is a high probability of finding particles with distinctly different velocities at the same location. Such behavior is known as the particle-trajectory crossing (PTC) in particle-fluid flows.

The numerical simulation of two-phase flows composed of a cloud of particles in a gas/fluid flow was the object of many studies in the past years, e.g., the dispersion of dusts and smokes [13], the modeling of biomedical flows [3,5] and combustion theory with various applications [1,2,19,26,36]. In order to model flows of this kind, one can essentially use two approaches: a kinetic one or a fluid one. In the kinetic model, the cloud of particles is described by a distribution function $f(t,x,\xi)$ which takes into account of the position x of a particle, and its velocity ξ. When function $f(t,x,\xi)$ is a Gaussian profile in terms of ξ, the kinetic model can be reduced to a fluid one. But for non-equilibrium flows, the solution method must be derived from the kinetic description since the fluid model can not handle locally multiple velocities observed in fluid-particle flows.

* Corresponding author.
E-mail addresses: hliu@iastate.edu (H. Liu), z2wang@math.ucsd.edu (Z. Wang), rofox@iastate.edu (R.O. Fox).

0021-9991/$ - see front matter © 2010 Elsevier Inc. All rights reserved.
doi:10.1016/j.jcp.2010.08.030

The main topic investigated in this work is the treatment of velocity dispersion by using the level set methodology. We will formulate our level set method for a non-collisional model equation governed by the Williams equation [36] for the number density function $f(t,x,\xi)$ as

$$\partial_t f + \xi \cdot \nabla_x f + \nabla_\xi \cdot (fF/m_p) = 0, \tag{1.1}$$

where F is the drag force acting on a particle, m_p is the particle mass. Note that extending f to include other variables (e.g., droplet temperature, chemical composition, collision, turbulent dispersion, etc.) is straightforward if the appropriate rate expressions are added to (1.1).The kinetic equation is often coupled with the following compressible fluid system

$$\partial_t \rho + \nabla_x \cdot (\rho u) = 0,$$
$$\partial_t (\rho u) + \nabla_x \cdot (\rho u \otimes u + P(\rho) I) = -\int F f d\xi,$$

where for perfect gases

$$P(\rho) = A\rho^\gamma, \quad A > 0 \quad \text{and} \quad \gamma > 1.$$

Local existence of solutions in the case of coupling with the compressible Euler equation was proved by Baranger and Desvillettes [4], where one can find references on previous works about fluid-kinetic coupling, in particular, when the fluid is modeled by one single equation [11].

Numerically instead of solving the full kinetic equation or classical moment equations [10,23], we capture velocity field of dispersed particles in phase space in an implicit manner via a level set approach. All particle velocities will be identified as the zero level sets of smooth functions.

In the context of fluid-particle flow, standard moment methods have found its difficulty treating systems with aggregation and breakage, and the Lagrangian particle tracking method has been widely used, say for sprays [12]. However, the treatment of dispersed phase introduces the additional complication of accounting for the dispersed-phase velocity. In the Lagrangian formulation, this is done by solving for the particle velocity as it transverses the (Eulerian) gas phase. Although accurate, this solution method is rather expensive and subject to statistical errors due to finite sample sizes. Similar to the quadrature method of moments (QMOM) developed in [30], recently the direct quadrature method of moments (DQMOM) [15–17,29] has been developed as an Eulerian method, which solves an Eulerian model where each quadrature node has its own velocity field. The number of moments needed to form a closed system of transport equations is $N(d+1)$ with N particle velocities in d spatial dimension. The comparison between the Lagrangian particle tracking method and the DQMOM method in [18] showed excellent agreement between quantities such as the droplet number density and mass density. The computational cost of the DQMOM is lower than the Lagrangian method, and this leads to an ongoing active development. However, complications occur when one needs to handle more particle clusters (larger N). These problems are amplified when solving a high dimensional problem.

In general, PTC does not occur at zero Stokes number, but can occur beyond a critical Stokes number when the particles are no longer able to follow the fluid. For small Stokes number, one usually explores the Eulerian model for gas-particle flows by taking the leading moments with a closure assumption $f = n\delta(\xi - v(t,x))$, which leads to a pressure-less system for

$$n(t,x) = \int_{R_\xi} f(t,x,\xi) d\xi, \quad nv = \int_{R_\xi} \xi f(t,x,\xi) d\xi.$$

We mention in passing that in the context of turbulence, the pressure-less model fails to reproduce the spreading of particles, even it is coupled with a turbulence model for the fluid. The partial remedy for this problem is to take a Gaussian-shape closure assumption (see [32] for related work)

$$f(t,x,\xi) = \frac{n(x,t)}{(2\pi\sigma(x,t))^{d/2}} \exp\left(\frac{|\xi - v(x,t)|^2}{2\sigma^2}\right),$$

where σ is particle velocity standard deviation, and by introducing additional diffusion terms in the governing kinetic equation. The simplest such model is

$$\partial_t f + \nabla_x \cdot (\xi f) + \nabla_\xi \cdot (fF/m_p) - \nabla_\xi \cdot (D\nabla_\xi f) = 0,$$

where D is a positive coefficient depending upon the properties of the fluid turbulence. We refer to [6,7,9,20] and references therein for modeling and computational aspects in this regime. We note that because of the closure assumption the system is not adapted to reproduce strongly non-equilibrium situations such as jet crossing, jet-wall interaction etc., and leads in those cases to non-physical solutions. Hence the level set method introduced in this article is not intended to handle the turbulence.

The main advantage of level set method over DQMOM is that it generates new velocities as needed, and thus is not limited to a fixed number N, For non-collisional case with initial distribution defined with discrete velocities, the level set method can give the exact evolution. In comparison, when the number of discrete velocities becomes greater than N, DQMOM will only yield an approximation that conserve $N(d+1)$ moments. The level set approach developed here handles more general closure assumptions and is well suited to study the PTC phenomena. This approach allows for large number of particle clouds in arbitrary dimension. One important feature of our method is that we use only one level set function to capture all possible

velocities, and any higher moments can be easily evaluated in a post-processing step if desired. There are also some limitations with the level set method, for example, the level set method works when the distribution is determined by a finite set of moments, one would face difficulty to initialize the level set function when the distribution generates an infinite set of independent moments.

Our level set method when applied to a problem confined in a bounded domain, wall boundary conditions need to be imposed so that to preserve the total mass flux. This can be done with reflective boundary conditions for smooth walls. But the level set method proposed in this article does not apply directly to "diffusive" (or rough) walls since in such cases the outgoing particle velocity is found from a distribution function (i.e. one value going in gives a continuous range of values going out).

We now conclude this section by outlining the rest of this paper: in Section 2 we formulate a level set description to capture the PTC phenomena. Discretization of level set equations is discussed in Section 3. Numerical results for some example applications are presented in Section 4. Some concluding remarks are given in Section 5.

2. Description of algorithm

2.1. Kinetic transport equations

In our study we shall consider the kinetic equation for a non-evaporating, mono-disperse particulate phase (with no collisions, secondary atomization, not turbulent dispersion). We shall denote the particle number density function by $f(t,x,\xi)$ in phase space $(x,\xi)\in\mathbb{R}^d\times\mathbb{R}^d$, and the force acting on a particle by F. The equations of transport are given by the Williams' equation [36]

$$\partial_t f+\xi\cdot\nabla_x f+\nabla_\xi\cdot(fF/m_p)=0, \tag{2.1}$$

where m_p denotes the mass of a particle. This model governs the particle evolution at the kinetic level in a d-dimensional physical space with particle velocity ξ and position x. All the relevant physics can in theory be included in this equation or its variant.

If one assumes that the particle density is much greater than the fluid density (e.g., solid or liquid particles suspended in gas), the expression for F is quite simple, and corresponds (in an initial force) to the sum of the drag force and the gravity force (often ignorable). Hence one has

$$F(u,\xi)=\frac{1}{2}\pi r^2\rho C_d|u(t,x)-\xi|(u(t,x)-\xi)+m_p g,$$

where u is the fluid velocity, r is the particle radius, ρ the fluid density, and C_d the particle drag coefficient given by the following correlation due to Schiller and Naumann [33]:

$$C_d=\frac{24}{Re}(1+Re^{2/3}),$$

with $Re=2\rho|u-\xi|r/\mu$ being the particle Reynolds number where μ is the dynamic viscosity of the fluid. Thus the basic form of the force F is given by

$$F=C(u(t,x)-\xi).$$

A conventional way to solve the kinetic equation is to use moment method to solve a system of moments. The moment system is often not closed, and an assumption on the shape of the number density function has to be made to form a closed system. For very small Stokes numbers, a simple assumption is

$$f=n\delta(\xi-v(t,x)).$$

One hence explores the Eulerian model for gas-particle flows by taking the leading moments with this closure assumption

$$n(x,t)=\int_{R_\xi} f(t,x,\xi)d\xi,\quad nv=\int_{R_\xi}\xi f(t,x,\xi)d\xi,$$

which leads to a pressure-less system

$$\begin{aligned}&\partial_t n+\nabla_x\cdot(nv)=0,\\&\partial_t(nv)+\nabla_x\cdot(nv\otimes v)=ng+\tfrac{n}{m_p}F(u,v).\end{aligned}$$

However, this model suffers a major drawback, by the closure assumption, it is unable to take into account the presence of particles with different velocities located at the same point. This can lead to non-physical results in the case of two crossing jets of particles, or in the case of a jet of particles impinging on a wall. This is not surprising since this model is not well-posed in the usual function spaces L^∞ or L^1 even in one-dimensional case, and cannot capture the particle-trajectory crossing (PTC) phenomena.

2.2. Level set description

Since $v(t,x)$ is expected to become multi-valued when particle trajectory crosses, conventional moment closure will incur inaccurate prediction when solving the kinetic equation. Instead, we shall use the level set technique to flexibly capture the particle-trajectory crossing. The usual closure method is derived by considering the concentrated data

$$f(t,x,\xi) = n(x,t)\delta(\xi - v(t,x)).$$

Such a concentration will propagate in phase space, with information concentrated only on a manifold. This observation leads to an effective level set description. The methodology follows from level set techniques developed for computing physical observables in high frequency wave propagation problems, see e.g. [25,24,27,28].

Our level set function is denoted as $\phi = \phi(t,x,\xi)$. Therefore all velocities are collectively represented as zero level set of ϕ, i.e.,

$$\phi(t,x,v(t,x)) \equiv 0.$$

This representation remains valid even $v(t,x)$ becomes multi-valued, while

$$v(x,t) \in \{\xi, \phi(t,x,\xi) = 0\}.$$

With this level set function we seek the solution of the following form

$$f(t,x,\xi) = \rho(t,x,\xi)\delta(\phi(t,x,\xi)),$$

where ρ serves to capture the weights of density distributions. Substitution of this ansatz into the William equation (2.1) leads to

$$\delta(\phi)a + \delta'(\phi)\rho b = 0, \tag{2.2}$$

where

$$\partial_t\rho + \xi\cdot\nabla_x\rho + \nabla_\xi\cdot(\rho F/m_p) = a,$$
$$\partial_t\phi + \xi\cdot\nabla_x\phi + F/m_p\cdot\nabla_\xi\phi = b.$$

In order to ensure (2.2) to hold for any (t,x,ξ) it suffices to take $a \equiv 0$ and $b \equiv 0$ for $\rho \not\equiv 0$. This leads to the key level set equation

$$\partial_t\phi + \xi\cdot\nabla_x\phi + F/m_p\cdot\nabla_\xi\phi = 0, \tag{2.3}$$

which can be computed near the neighborhood of $\phi = 0$, as well as a transport equation for the weight ρ:

$$\partial_t\rho + \xi\cdot\nabla_x\rho + \nabla_\xi\cdot(\rho F/m_p) = 0. \tag{2.4}$$

Note that a sub-domain where $\rho = 0$ indicates no particles in that region, so there is no need to track the velocity field.

We thus can state the following.

Theorem 2.1. *Let ϕ be the solution to (2.3) subject to initial data $\phi(0,x,\xi)$, and ρ be the solution to (2.4) with initial data $\rho(0,x,\xi)$, then*

$$f(t,x,\xi) = \rho(t,x,\xi)\delta(\phi(t,x,\xi))$$

is the solution of the William Eq. (2.1) *with initial distribution of the form $\rho(0,x,\xi)\delta(\phi(0,x,\xi))$.*

2.3. Initialization

Special care must be taken when constructing initial data for the above level set equation and the density transport equation. Let Ω be a bounded domain, which contains a finite number (assumed to be K) of particle clouds. Let each set of particle clouds be denoted by J_i with $\cup_{i=1}^N J_i \subset \Omega$, associated with particle density $\rho_i(x)$ and velocity $u_i(x)$. The initial distribution of particles can be expressed as an expansion of the number density function in a sum of weighted delta functions in phase spaces [16]:

$$f(0,x,\xi) = \sum_{i=1}^{K}\rho_i(x)\chi_{J_i}(x)\delta(\xi - u_i(x)),$$

where $\chi_{J_i}(x)$ denotes the characteristic function of $J_i \subset \Omega$.

From this expression it follows that for $x \in J_k$

$$\rho_k(x) = \int f(0,x,\xi)d\xi, \quad u_k(x) = \frac{\int \xi f(0,x,\xi)d\xi}{\int f(0,x,\xi)d\xi}.$$

This is consistent with the usual formulation of moments, thus we say the above choice of initial distribution is admissible.

We now turn to construction of a level set function $\phi(0,x,\xi)$ so that

$$\bigcup_{i=1}^{K}\{(x,\xi), x\in J_i, \xi = u_i(x)\} = \{(x,\xi), \phi(0,x,\xi)=0\}.$$

The classical level set method initiated in [31] has been successful is computing moving curves (or surfaces) in physical space, here we develop the level set method in phase space. Moreover, in current application the zero level set is not necessarily a closed curve or surface, but can be just a set of collected points or regions.

Note that the initial choice of $\phi(0,x,\xi)$ is not unique. Unless otherwise specified, we shall use the distance function to initialize the velocity field as follows:

$$\phi_0(x,\xi) := \phi(0,x,\xi) = \min_i \min_{y\in J_i} \sqrt{|x-y|^2 + |\xi - u_i(y)|^2}. \tag{2.5}$$

The cost for a direct computation is about $O(KM^{2d}M_J^d)$, where M is the number of grid points in each direction, and M_J denotes the number of grid points in the set J_i where particle clouds are located. The complexity is small if there is only small number of particle clouds.

Next we construct a density weight function $\rho(0,x,\xi) > 0$ so that

$$\rho(0,x,\xi)\delta(\phi(0,x,\xi)) = \sum_{i=1}^{K} \rho_i(x)\chi(J_i)\delta(\xi - u_i(x))$$

in distributional sense. We take

$$\rho_0(x,\xi) := \rho(0,x,\xi) = \sum_{i=1}^{K} \rho_i(x)|\partial_\xi \phi_0|_{\xi=u_i(x)}\chi(J_i) \tag{2.6}$$

so that for any smooth test function $V \in C_0^\infty(\mathbb{R}^d)$ we have

$$\int \rho_0(x,\xi)\delta(\phi_0(x,\xi))V(\xi)d\xi = \sum_{i=1}^{K} \rho_i(x)\chi(J_i)V(u_i).$$

2.4. Post-processing

Once having solved the above equations we are in a position to evaluate the desired physical quantities. The zero level set of $\phi(t,x,\xi)$ gives multiple velocities at location x and time t:

$$v(t,x) \in \{\xi, \phi(t,x,\xi)=0\}.$$

Note that as time evolves ϕ can become flat and small simultaneously, this would bring difficulties to identify a sharp set of zeros of ϕ. In this case, higher order interpolation may be used to determine the zero level set.

The velocity moments of any order can be obtained in the following post-precessing step, for example,

$$M^0(t,x) = \bar{n}(x,t) = \int_{R_\xi} \rho\delta(\phi)d\xi, \quad M_i^1(t,x) = \int_{R_\xi} \xi_i\rho\delta(\phi)d\xi.$$

It can be shown as in [28] that for N velocities v_α with density n_α, we have

$$\bar{n}(x,t) = \sum_{\alpha=1}^{N} n_\alpha, \quad \bar{v} = \frac{\sum_{\alpha=1}^{N} n_\alpha v_\alpha}{\sum_{\alpha=1}^{N} n_\alpha}.$$

Note that using moment closure method one needs at least $N(d+1)$ moments to resolve the desired number of velocities and associated densities. The main advantage of the level set method described above is its ability to capture all emerging velocities and densities in an implicit manner. Moments of any desired order can be evaluated in a post-processing step. It is demonstrated in the numerical examples.

2.5. Summary

We can now summarize our algorithm.

Step 1. Initialize $\phi_0 = \phi_0(x,\xi)$ to be a distance function to the graph of the initial velocity distribution of particles. With ϕ_0 so selected, we take initial density $\rho_0(x,\xi)$ as defined in (2.6). In some situations, this step can be easier. For example when initial velocity is a given continuous function, we simply take $\phi_0 = \xi - u_0(x)$, associated with $\rho_0 = \rho_0(x)$.

Step 2. Solve the level set equation

$$\partial_t\phi + \xi\cdot\nabla_x\phi + F/m_p\cdot\nabla_\xi\phi = 0,$$

for one time step. The computation is done in the neighborhood of $\phi = 0$. Denote the update ϕ by ϕ^{n+1}.

Step 3. Solve the transport equation

$$\partial_t\rho + \nabla_x\cdot(\xi\ \rho) + \nabla_\xi\cdot(\rho F/m_p) = 0,$$

to obtain ρ^{n+1}.

Step 4. We have now advanced one time step. The zero level set of ϕ^{n+1} gives the new multiple velocity, and the density weight ρ^{n+1}. Repeat steps 2 and 3.

Step 5. At the final time, multiple velocities are determined by the contour plot $\phi = 0$ for any (t,x).

Step 6. Evaluation of physical quantities: total density and mean velocity of particles.

$$\bar{n}(x,t) = \int_{R_\xi}\rho\delta(\phi)d\xi, \quad \bar{v} = \int_{R_\xi}\xi\rho\delta(\phi)d\xi/\bar{n}(x,t). \tag{2.7}$$

For an accurate evaluation of above integrals, it is essential to approximate δ correctly over the grid. This amounts to the selection of the approximate kernel and the regularization parameter in relation to both the given grid geometry and the gradient of the level set functions, as shown in [14,25]. Indeed, improper use of the approximate Dirac delta function may lead to artificial numerical oscillations. In our simulation we approximate the Dirac $-\ \delta$ function by

$$\delta_\epsilon^{\cos}(x) = \frac{1}{2\epsilon}\left(1 + cos\left(\frac{\pi x}{\epsilon}\right)\right)I_{[-\epsilon,\epsilon]}, \tag{2.8}$$

and take $\epsilon = m\ \max(|\nabla_p\phi|,1)h$ with $m = 1$, with h being the spatial step size. Such a choice is a modification of that used in [25].

3. Discretization

Because of the transport form of the system for the level set function, and the conservative form for the density weight, we shall use finite difference and finite volume method for these two systems respectively. For the sake of clarity, let us begin by considering the one-dimensional in x case, the multi-dimensional extension being straightforward.

A uniform mesh will be used for the density weight and the level set function. With Δx and $\Delta\xi$ as the mesh size in x and ξ direction,

we define

$$\begin{aligned}
&x_i = i\Delta x, \xi_j = j\Delta\xi,\\
&\rho_{i,j} = \rho(x_i,\xi_j),\\
&\phi_{i,j} = \phi(x_i,\xi_j),\\
&i = 0,\ldots M-1,\\
&j = 0,\ldots N-1.
\end{aligned}$$

3.1. Second order finite difference (FD) scheme for the level set equation

We use a second order TVD-Range-Kutta [34] method for evolving the level set equation in time, and high-resolution upwind method for spatial transport. In order to present the numerical scheme in explicit manner, here and in what follows we use following notations: $D_x^\pm$ denote finite difference operators in x-direction.

$$D_x^+\phi_j = \frac{\phi_{j+1}-\phi_j}{\Delta x} = D_x^-\phi_{j+1}, \quad D_x^0\phi_j = \frac{\phi_{j+1}-\phi_{j-1}}{2\Delta x}.$$

The difference operator in ξ direction is similarly defined. Here and in what follows we shall use the following notation

$$g^+ = \frac{1}{2}(|g|+g), \quad g^- = \frac{1}{2}(g-|g|)$$

to denote both positive and negative part of the quantity, respectively. The solution is firstly advanced to the full time step using the forward Euler method as a prediction

$$\phi_{j,k}^* = \phi_{j,k}^n - \Delta t L[\phi]_{j,k}^n, \tag{3.1}$$

where

$$L[\phi] := \left[\xi_k^+\widetilde{D}_x^-\phi + \xi_k^-\widetilde{D}_x^+\phi + F^+\widetilde{D}_\xi^-\phi + F^-\widetilde{D}_\xi^+\phi\right].$$

Here Δt is the time step, j and k denote the grid indices and n denotes the time interval. The difference operator $\widetilde{D}$ is restricted by limiters to preserve certain monotonicity. In our computation we use a second order ENO (essentially nonoscillatory) limiter [22,35]. Define

$$m(a,b) = \begin{cases} a & \text{if} |a| \leqslant |b|, \\ b & \text{otherwise}. \end{cases}$$

We now have for $h = \Delta x$

$$\widetilde{D}_x^- \phi_j = D_x^- \phi_j + hm(D_x^+ D_x^- \phi_{j-1}, D_x^+ D_x^- \phi_j)/2,$$
$$\widetilde{D}_x^+ \phi_j = D_x^+ \phi_j - hm(D_x^+ D_x^- \phi_j, D_x^+ D_x^- \phi_{j+1})/2.$$

The numerical solution at next time step is determined by

$$\phi_{j,k}^{n+1} = \frac{1}{2}\phi_{j,k}^{n} + \frac{1}{2}\phi_{j,k}^{*} - \frac{\Delta t}{2} L[\phi^*]. \tag{3.2}$$

3.2. Second-order finite volume (FV) scheme for density transport

Let $I_{j,k} = I_j \times I_k$be a control volume with $I_j = [x_{j-1/2}, x_{j+1/2}]$ and $I_k = [\xi_{k-1/2}, \xi_{k+1/2}]$; and $\rho_{j,k}$ be the cell average over $I_{j,k}$. In each $I_{j,k}$, the solution representative is a first order polynomial

$$p[\rho]|_{I_{j,k}} = \rho_{j,k} + s'_{j,k}(x - x_j) + s\grave{}_{j,k}(\xi - \xi_k),$$

with minmod slopes [21] chosen as

$$s'_{j,k} = mm\left(D_x^+ \rho_{j,k}, D_x^- \rho_{j,k}\right), \quad s\grave{}_{j,k} = mm\left(D_y^+ \rho_{j,k}, D_y^- \rho_{j,k}\right).$$

Thus the semi-discrete scheme can be written as

$$\frac{d}{dt}\rho_{j,k} + \frac{(\widehat{\xi\rho})_{j+1/2,k} - (\widehat{\xi\rho})_{j-1/2,k}}{\Delta x} + \frac{(\widehat{F\rho})_{j,k+1/2} - (\widehat{F\rho})_{j,k-1/2}}{\Delta \xi} = 0. \tag{3.3}$$

Classical upwind numerical fluxes are adopted as

$$(\widehat{\xi\rho})_{j+1/2,k} = \xi_k^+ \left(\rho_{j,k} + \frac{\Delta x}{2} s'_{j,k}\right) + \xi_k^- \left(\rho_{j+1,k} - \frac{\Delta x}{2} s'_{j+1,k}\right), \tag{3.4}$$

$$(\widehat{F\rho})_{j,k+1/2} = F^+(t, x_j, \xi_{k+1/2}) \left(\rho_{j,k} + \frac{\Delta y}{2} s\grave{}_{j,k}\right) + F^-(t, x_j, \xi_{k+1/2}) \left(\rho_{j,k+1} - \frac{\Delta y}{2} s\grave{}_{j,k+1}\right). \tag{3.5}$$

Now the semi-discrete scheme is a closed ODE system for cell averages $\{\rho_{j,k}\}$. A second order Runge–Kutta method is applied for time discretization.

3.3. Multi-dimensional extension

The multidimensional extension of the scheme we just described follows naturally using dimension-by-dimension handling. Indeed, the level set equation and density transport equation have already been derived for multiple dimensions, and the computation of numerical fluxes in multi-dimensional case is essentially the same as described above. Details are omitted.

4. Numerical results for example applications

In this section we apply our level set algorithm to non-equilibrium fluid-particle flows in order to illustrate its ability to handle non-trivial problems. We will consider the case without drag force (or equivalently with infinite Stokes number) and the case with given drag forces for a range of Stokes numbers. The complex case with the drag-force computed from a coupled gas dynamic system will be considered elsewhere.

4.1. One-dimensional test cases

4.1.1. Impinging particles

The first flow that we consider is one-dimensional with two particle "packets" moving in opposite directions. The particles are collisionless and not affected by any drag forces.

For these two particles, we give initial density and velocity as follows:

$$\rho_0(x) = \frac{1}{3}\delta(x-0.25) + \frac{2}{3}\delta(x-0.75), \quad u_0(0.25) = 1, \quad u_0(0.75) = -1.$$

In the simulation computation domain is chosen as $[0,1]\times[-1.1,1.1]$. In the initialization step we take $f(0,x,\xi) = \rho_0(x,\xi)\delta(\phi_0(x,\xi))$, where

$$\phi_0(x,\xi) = \xi - u_0^\epsilon(x),$$
$$\rho_0(x,\xi) = \rho_0^\epsilon(x),$$

where $(\rho_0^\epsilon, u_0^\epsilon)$ are the approximation of (ρ_0, u_0) using cosine kernel, i.e.,

$$\rho_0^\epsilon = \frac{1}{3}\delta^\epsilon(x-0.25) + \frac{2}{3}\delta^\epsilon(x-0.75), \delta^\epsilon(y) = \frac{1}{2\epsilon}(1+cos(\pi y/\epsilon))I_{[-\epsilon,\epsilon]}(y)$$

and

$$u_0^\epsilon(x) = \begin{cases} 1 & |x-0.25| \leqslant \epsilon, \\ -1 & |x-0.75| \leqslant \epsilon, \end{cases}$$

where ϵ is the same as that used to approximate the two Dirac delta functions. A constant extension is used to impose the boundary condition. The two packets will thus eventually collide at $t = 0.25$. The results are shown in Fig. 1 at time 0.1, 0.2, 0.3 and 0.4. We see two particles before and after collision at time 0.2 and 0.3, respectively. This example illustrates the capability of our numerical method in capturing the PTC phenomenon in a simple setting.

4.1.2. Three clouds of particles

This example illustrates the crossing behavior of three clouds of particles. The initial setting is as follows:

$$u_0(x) = \begin{cases} 0.5, & x \leqslant 0.2, \\ 0, & 0.4 \leqslant x \leqslant 0.6, \\ -0.5, & x \geqslant 0.8, \end{cases}$$
$$\rho_0(x) = 0.5\chi_{x\leqslant 0.2} + 1.0\chi_{0.4\leqslant x\leqslant 0.6} + 1.5\chi_{x\geqslant 0.8}.$$

The computation domain is $[0,1]\times[-0.75,0.75]$. The distance function is used to initialize ϕ. A constant boundary conditionis used to mimic the particle flow getting in/out of the computational domain. By characteristic method one can easily show that at time $t = 0.4$, particles will collide at $x = 0.6$ and $x = 0.8$. We present the density at $t = 0.1, 0.5, 0.7, 1.0$ in Fig. 2 before and after collision. Before collision, at $t = 0.1$, we see the movement of the particle clouds. After the first collision at $x = 0.6$ and $x = 0.8$, we observe the superposition of the density of two clouds at time $t = 0.5$. After the second collision at $x = 0.5$, we see the superposition of the density of three clouds at $t = 0.7, 1.0$. These observations are confirmed by the velocity plots as well in Fig. 2.

This example shows that the level set method generate more velocities as needed. In comparison, the DQMOM method will only yield an approximation that conserve $2N$ moments when number of velocities is bigger than a fixed N.

4.1.3. Finite stokes number

The previous two examples simulate the free motion (infinite Stokes number) of clouds of particles without coupling with fluid. They demonstrate the capability and simplicity of our level set method in describing the non-equilibrium particle flows with arbitrary number of phases. The fluid is added to the next example to simulate the effect of both transport and drag. Different Stokes numbers are tested to comply with different physical properties of the fluid. For all the Stokes numbers, the initial particle density is given by

$$\rho(0,x) = e^{-25x^2}$$

and the initial particle velocity is

$$u(0,x) = -\sin(2\pi x)|\sin(2\pi x)|.$$

We test our method in the following simplified model

$$\partial_t f(t,x,\xi) + \xi\cdot\nabla_x f + \nabla_\xi\cdot(Ff) = 0, \tag{4.1}$$
$$\rho_f(\partial_t u + uu_x) = -\int m_p F(t,x,\xi) f d\xi, \tag{4.2}$$

where ρ_f denotes the fluid density and m_p is the droplet mass. Both ρ_f and m_p are assumed to be *1* for simplicity.The initial fluid velocity is set to be a shock moving to the right, i.e.,

$$u(0,x) = H(-x),$$

where $H(x)$ is the heaviside function. The linear drag force is hence

$$F(t,x,\xi) = (u(t,x)-\xi)/S_t, \quad S_t = 0.1, 1, 10, \cdots.$$

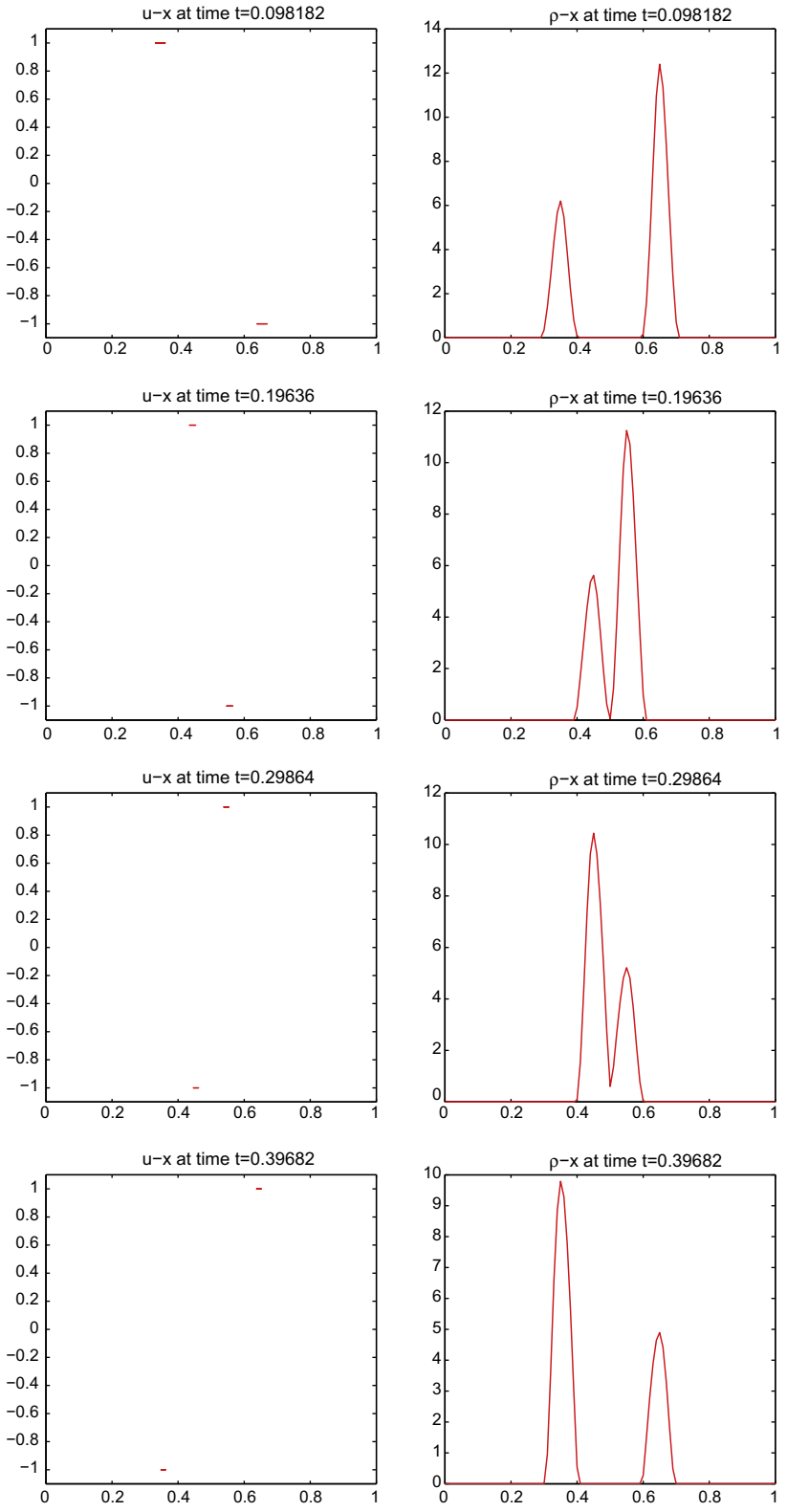

Fig. 1. Multiple velocity and averaged density at time about 0.1, 0.2, 0.3 and 0.4.

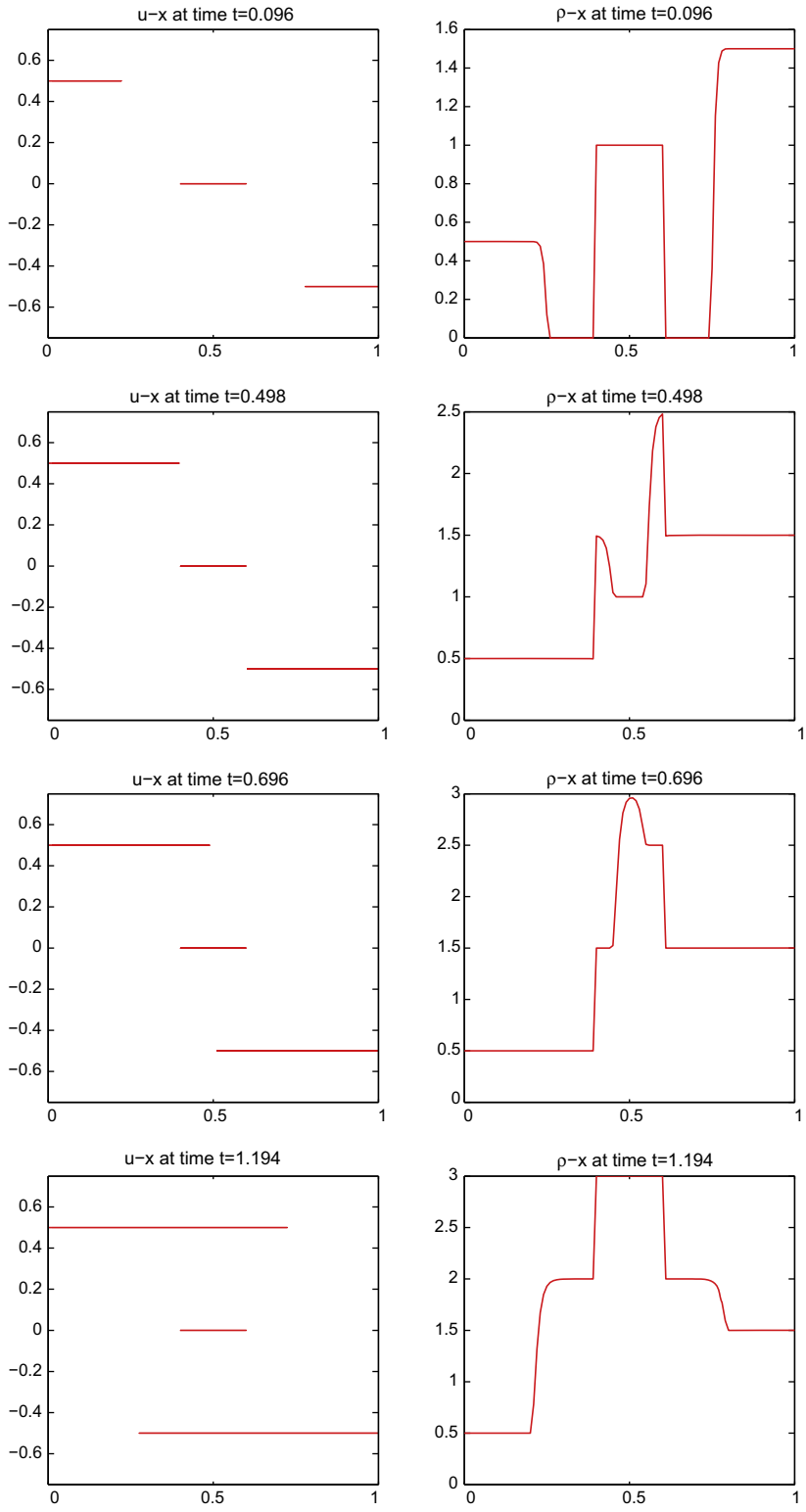

Fig. 2. Multiple velocity and total density at time about 0.1, 0.5, 0.7 and 1.0.

The fluid dynamic Eq. (4.2) is solved with a second order Runge–Kutta temporally and a finite volume scheme with a second order ENO flux limiter spatially. Here we simply take $\phi(0,x,\xi) = \xi - u(0,x)$ since particles are everywhere. A constant

extension boundary condition for fluid velocity and particle density is used, while a periodic boundary condition is employed for the particle velocity.

4.1.3.1. Case 1: Stokes number $S_t = 0.1$. When $S_t = 0.1$, the drag force is strong, so the particle will follow the fluid closely and no particle will cross at beginning. However, after a short time the PTC starts to appear. Note that for small Stokes number, the fluid velocity changes rapidly in some region (near $x = 0$ at time $t = 0.2$). This is caused by the multiple particle velocity near $x = 0$. Due to the large drag force F, the fluid will not maintain the shock profile. At time $t = 0.5$, some oscillation also exhibits in the fluid. See in Fig. 3 for details.

4.1.3.2. Case 2: Stokes number $S_t = 1$. When S_t changes to *1*, the drag force becomes weaker, we see particle crossing each other as shown in Fig. 4. Observe that particle distribution becomes smoother, and the fluid is less affected by particles. However, near the shock, interaction between fluid and particle is still distinctly visible.

4.1.3.3. Case 3: Stokes number $S_t = 10$. When $S_t = 10$, the drag force is small, so the particles respond to the fluid very slowly and behave like the ones in free motion as we see in Fig. 5. Since the particle is less affected by the fluid, the particle trajectories cross in the simulation. We observe five particle velocities at time $t = 0.5$. This is also confirmed by the fluid velocity, which is close to the movement of shock. Due to the complex structure of the particle velocity, more nodes are needed if quadrature-based moment method is used. This example shows that initial uni-mode velocity will become multi-valued when PTC happens due to the interaction between fluid and particles. The level set method we use here does capture all emerging velocity modes.

4.2. Two-dimensional test cases

4.2.1. Crossing particle jets

In this example, we demonstrate the ability of the level set method to capture particle crossing trajectories in two dimensional flows with infinite Stokes number particles.

Restricted in a unit box $\{x| \quad |x_1| \leqslant 0.5, |x_2| \leqslant 0.5\}$, two jets are initially concentrated in two separate regions

$$J_1 = \{x|0.25 \leqslant x_1 \leqslant 0.5, |x_2| \leqslant 0.025\}, \quad J_2 = \{x||x_1| \leqslant 0.05, -0.5 \leqslant x_2 \leqslant -0.35\}.$$

The initial setting for these two jets can be described as

$$\rho_0(x) = 20\chi(J_1) + 20\chi(J_2), \quad u_0(x) = [-1, 0]\chi_{J_1} + [0, 1]\chi_{J_2}.$$

Initial data for the distribution is $f_0(x,\xi) = \rho_0(x,\ \xi)\delta(\phi_0(x,\xi))$. A distance function in (2.5) is used to initialize $\phi(0,x,\xi)$. $\rho(0,x,\xi)$ is initialized as $\rho_0(x)|\nabla_\xi\phi(0,x,\xi)|$. An impinging boundary condition is used to represent incoming particles in x direction.

We know that when $t = 0.25$ two jets start to collide. We can clearly see the collision at time $t = 0.3$. When $t = 0.5$ two jets have crossed each other. Fig. 6 illustrates the time evolution of particle number density for crossing jets. Here the solid lines represent the exact solutions while the red dashed lines represents the numerical solutions. We see that the level set method indeed captures all crossings of particle trajectories.

Fig. 7 shows the density at time 0.5. Besides some numerical viscosity at the tips of the particle flows, it validates the quantitative correctness in recovering the particle density.

4.2.2. Particle wall rebound

In this example, we consider a particle flow bouncing off a reflective wall. Still restricted in a unit box $\{x| \quad |x_1| \leqslant 0.5, |x_2| \leqslant 0.5\}$, a particle jet is initially concentrated in the region

$$J = \{x| -0.5 \leqslant x_1 \leqslant -0.1, -0.55 \leqslant x_1 + x_2 \leqslant -0.45\}.$$

The initial setting for distribution is given by

$$f_0(x,\xi) = \rho_0(x)\delta(\xi - u(x)),$$

where

$$\rho_0(x) = \chi_J, \quad u = [1 \quad -1]\chi_J.$$

The particle with velocity $[1\ -1]$ will be bounced off the wall $W_r = \{x| \quad x_2 = -0.5\}$ with velocity $[1 \quad e]$, $0 \leqslant e \leqslant 1$. Most moment closures use the average velocity $[1 \quad (e-1)/2]$ for convective transport, they are not able to reflect particles from the wall. At the wall we use a reflective boundary condition

$$f(t,x,\xi_{\text{in}}) = J^{-1}f(t,x,\xi_{\text{out}}),$$

where

$$\xi_{\text{out}} = \xi_{\text{in}} - \alpha(\xi_{\text{in}} \cdot v(x))v(x)$$

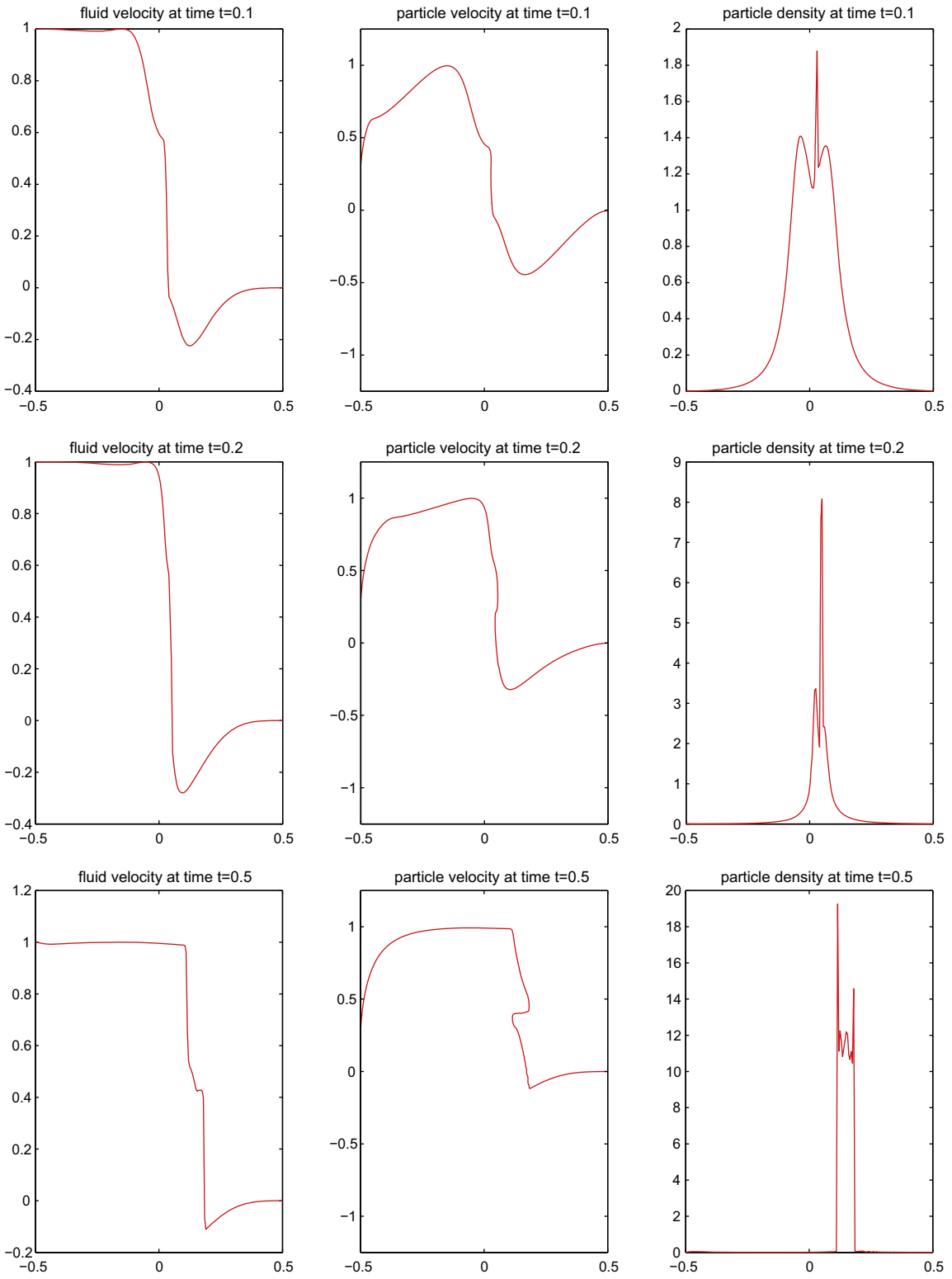

Fig. 3. Velocity, particle velocity and particle density at time $t = 0.1$, 0.2 and 0.5 for $S_t = 0.1$.

with $v(x)$ the unit outer normal vector at the point $x \in \partial\Omega$, α a reflective parameter and $J = \det(\frac{\partial \xi_{\text{out}}}{\partial \xi_{\text{in}}})$. Here the factor J^{-1} is used to conserve the total mass.

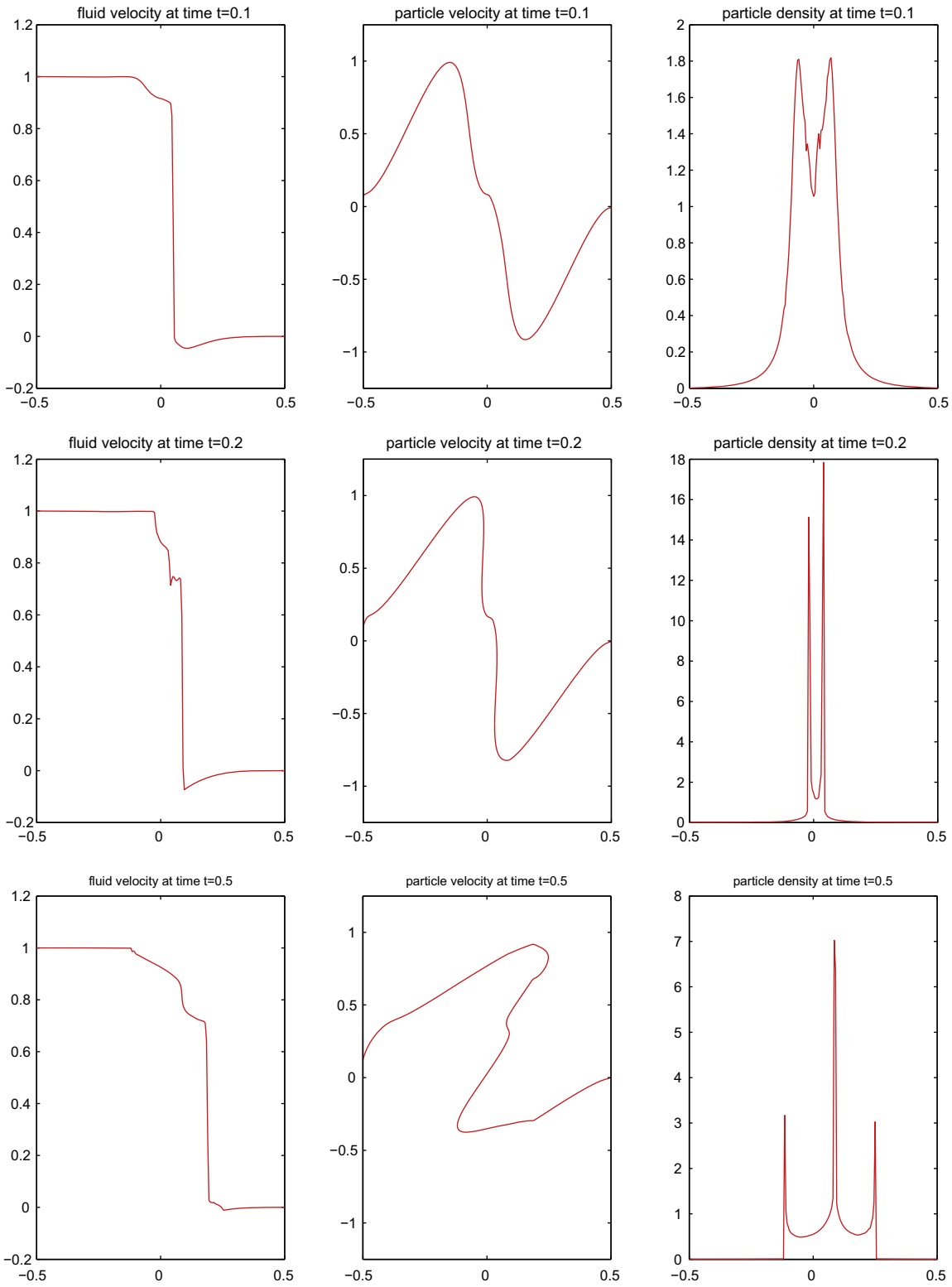

Fig. 4. Velocity, particle velocity and particle density at time $t = 0.1$, 0.2 and 0.5 for $S_t = 1$.

In this example $v(x) = (0, -1)^\top$. Thus $\alpha = 1 + e$ and $J = |-1 - \alpha|v|^2| = e$, which indicates that when $e = 0$ mass accumulates at the wall. Such a reflective boundary condition can be built in our level set formulation in a similar way to that introduced in [8].

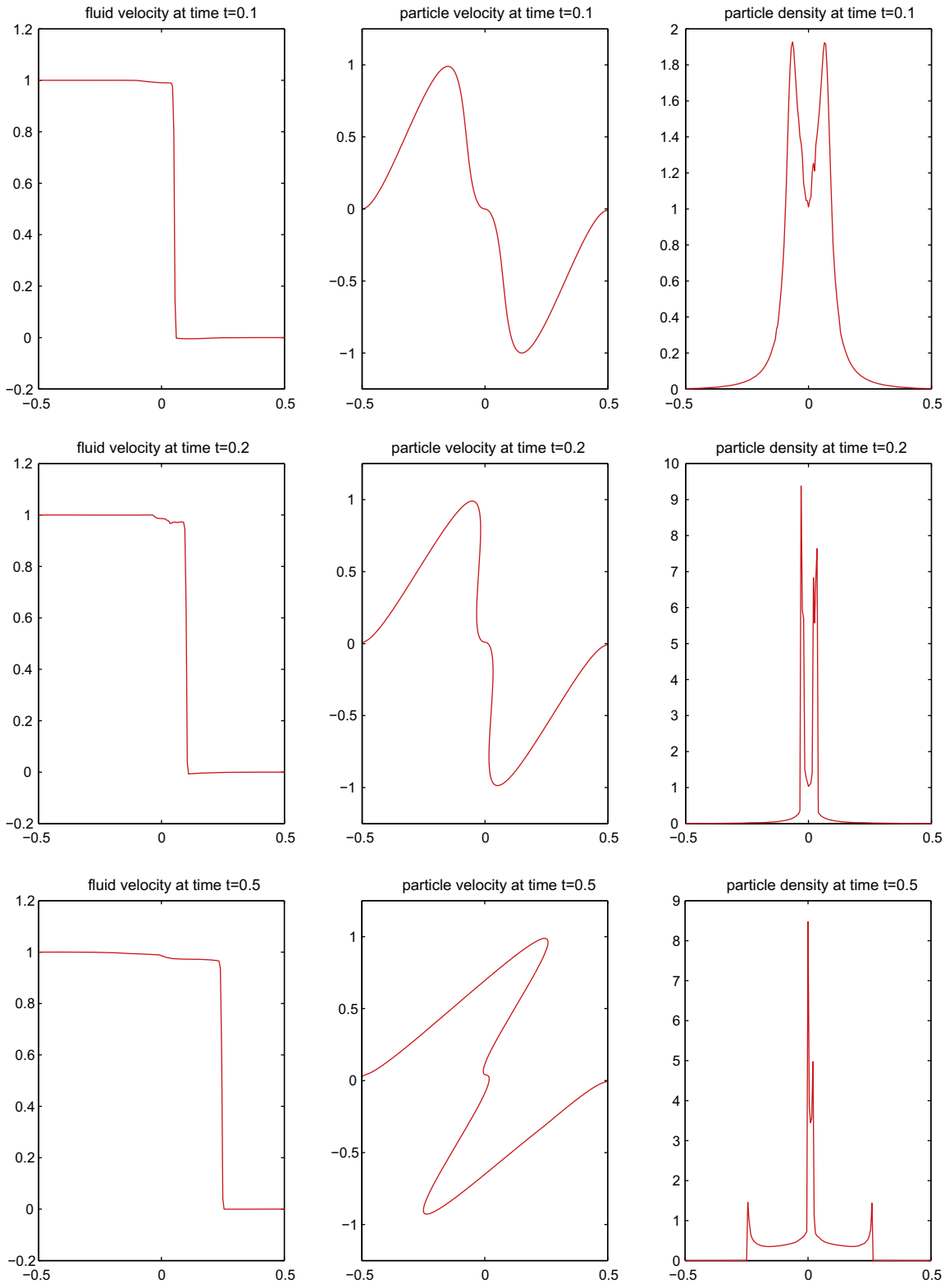

Fig. 5. Fluid velocity, particle velocity and particle density at time $t = 0.1$, 0.2 and 0.5 for $S_t = 10$.

At the reflective wall $W_r = \{x| \quad x_2 = -0.5\}$, we hence use following boundary conditions for both ϕ and ρ, respectively

$$\phi(t,x,\xi_{\text{in}}) = \phi(t,x,\xi_{\text{out}}), \quad \rho(t,x,\xi_{\text{in}}) = \rho(t,x,\xi_{out})/e, \quad x \in W_r,$$

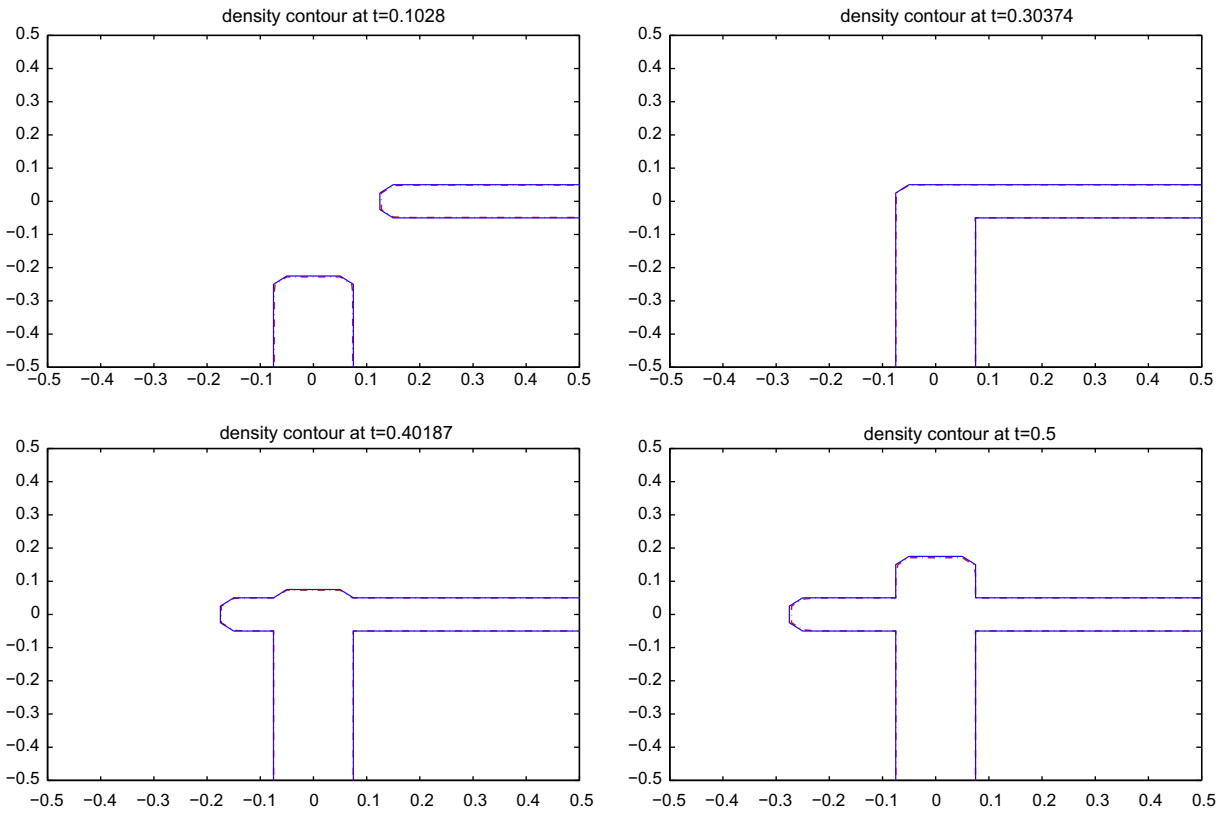

Fig. 6. Density contour at time about 0.1, 0.3 and 0.5.

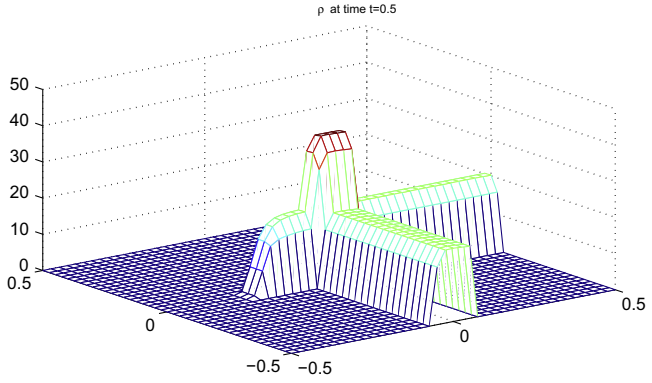

Fig. 7. Density at time 0.5.

where

$$\xi_{\text{in}} = (\xi_1, \xi_2), \quad \xi_{\text{out}} = (\xi_1, -e\xi_2).$$

For discretization of the computational box, we use hyper-rectangular meshes with uniform spatial step sizes Δx_1, Δx_2, $\Delta\xi_1$ and $\Delta\xi_2$. Numerically, we need to approximate level set derivatives at both incoming and rebounding walls.

At the incoming wall $W_i = \{x | x_1 = -0.5\}$, we use backward difference between the boundary point $(-0.5, x_2)$ and a ghost point $(-0.5 - \Delta x_1, x_2)$ outside the domain to determine $D^-_{x_1}\phi(-0.5, x_2, \xi)$. The value of ϕ at the ghost point is obtained from an extrapolation and interpolation procedure: assume $\Delta x_1 \leqslant \Delta x_2$, a constant extrapolation along the incoming flow direction $(1, -1)^\top$ gives

$$\phi(-0.5 - \Delta x_1, x_2, \xi) = \phi(-0.5, x_2^*, \xi)$$

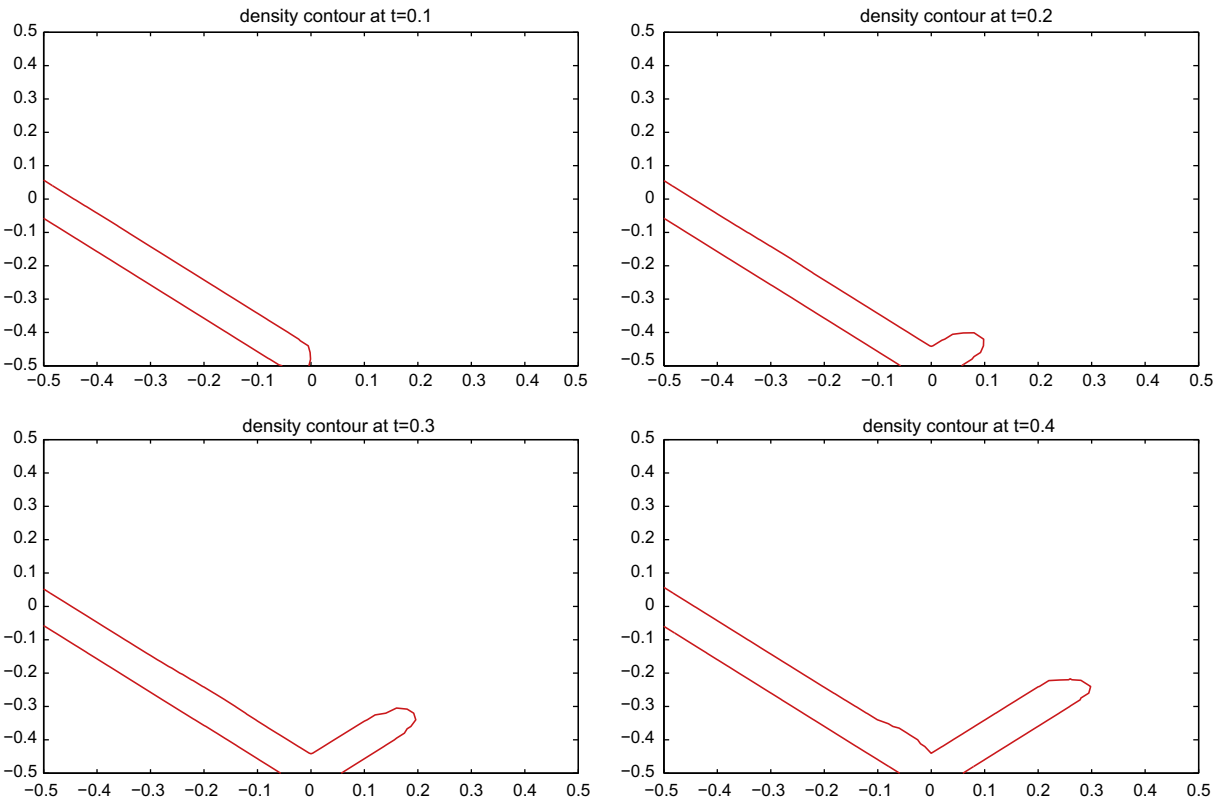

Fig. 8. Density contour at time about 0.1, 0.2, 0.3 and 0.4.

with $x_2^* = x_2 - \Delta x_1$. Using interpolation based on both $\phi(-0.5,x_2,\xi)$ and $\phi(-0.5,x_2-\Delta x_2,\xi)$ we obtain

$$\phi(-0.5,x_2^*,\xi) = \left(1-\frac{\Delta x_1}{\Delta x_2}\right)\phi(-0.5,x_2,\xi) + \frac{\Delta x_1}{\Delta x_2}\phi(-0.5,x_2-\Delta x_2,\xi).$$

Thus we take

$$D_{x_1}^- \phi(-0.5,x_2,\xi_1,\xi_2) = \frac{\phi(-0.5,x_2,\xi_1,\xi_2) - \phi(-0.5,x_2^*,\xi_1,\xi_2)}{\Delta x_1}.$$

At the rebounding wall W_r, we connect both outgoing velocity and its reflective counterpart through the reflective boundary condition for ϕ so that the reflective velocity is captured. In this example, the velocity in x_2 direction changes from ξ_2 to $-e\xi_2$ after reflection. A periodic extension is then used to approximate the level set derivative with respect to x_2 as

$$D_{x_2}^- \phi(x_1,-0.5,\xi_1,\xi_2) = \frac{\phi(x_1,-0.5,\xi_1,-e\xi_2) - \phi(x_1,0.5-\Delta x_2,\xi_1,-e\xi_2)}{\Delta x_2}.$$

The density contours are plotted in Fig. 8. It clearly shows the movement and rebouncement of the particle flow. This example demonstrates the adaptable capacity of the level set method to incorporate physical conditions such as particle rebound off walls.

5. Concluding remarks

A level set approach for kinetic equations of particle clouds has been derived and verified for non-equilibrium, dilute, fluid-particle flows. For non-collisonal case, the method can successfully handle flows with particle-crossing trajectories and thus is able to compute accurately particle velocity statistics in an Eulerian framework. The main advantage of level set method over DQMOM is that it generates new velocities as needed, and thus is not limited to a fixed number N. For non-collisional case with initial distribution defined with discrete velocities, the level set method can give the exact evolution. In comparison, when the number of discrete velocities becomes greater than N, DQMOM will only yield an approximation that conserve $N(d+1)$ moments. One important feature of the level set method is that it requires only one level set

function to capture all possible velocities, and any higher moments can be evaluated in a post-processing step if desired; thus the level set approach developed in this paper is well suited to study the PTC phenomena.

We point out that the level set method developed here is ideal mainly for the non-collisional, non-diffusive cases and when initial distributions generate only finite number of moments. It would be a challenging task to extend the present approach to handle more complicate situations such as cases with collision and/or diffusion. Our level set method applies also to particles rebound off smooth walls; but not directly suitable to diffusive (or rough) walls.

Finally, in addition to applications involving dispersed-phase flows, the proposed methodology should find use in some other applications governed by non-collisional kinetic equations.

Acknowledgments

The authors thank the anonymous referees who provided valuable comments resulting in improvements in this paper. Liu's research was partially supported by the National Science Foundation under Kinetic FRG grant DMS07-57227 and grant DMS09-07963.

References

[1] A. Amsden, J. Ramshaw, P. ORourke, J. Dukowicz, A computer program for two- and three-dimensional fluids flow with chemical sections and fuel sprays, Los Alamos (1985).
[2] C. Baranger, Modelling of oscillations, breakup and collisions for droplets: the establishment of kernels for the 3T.A.B. model, Math. Models Meth. Appl. Sci. 14 (5) (2004) 775–794.
[3] C. Baranger, L. Boudin, P.-E. Jabin, S. Mancini, A modeling of biospray for the upper airways, in: CEMRACS 2004—Mathematics and Applications to Biology and Medicine, vol. 14 of ESAIM Proc., (electronic), EDP Sci., Les Ulis, 2005, pp. 41–47.
[4] C. Baranger, L. Desvillettes, Coupling Euler and Vlasov equations in the context of sprays: the local-in-time, classical solutions, J. Hyperbolic Differ. Equ. 3 (1) (2006) 1–26.
[5] L. Boudin, L. Weynans. Spray impingement on a wall in the context of the upper airways, in: CEMRACS 2004—mathematics and applications to biology and medicine, vol. 23 of ESAIM Proc., EDP Sci., Les Ulis, 2008, pp. 1–9.
[6] J. Carrilo, T. Goudon, Stability and asymptotic analysis of a fluid-particles interaction model, Commun. Part. Differ. Equ. 31 (2006) 1349–1379.
[7] J. Carrilo, T. Goudon, P. Lafitte, Simulation of fluid and particles flows: asymptotic preserving schemes for bubbling abd flowing regimes, J. Comput. Phys. 227 (2008) 7929–7951.
[8] L.-T. Cheng, M. Kang, S. Osher, H. Shim, Y.-H. Tsai, Reflection in a level set framework for geometric optics, CMES Comput. Model. Eng. Sci. 5 (4) (2004) 347–360.
[9] K. Desjardins, P. Villedieu, A hierarchy of models for turbulent dispersive two-phase flows derived from a kinetic equation for the joint particle-gas, Commun. Math. Sci. 5 (2007) 331–353.
[10] R.B. Diemer, J.H. Olson, A moment methodology for coagulation and breakage problems: part 2 - moment models and distribution reconstruction, Chem. Eng. Sci. 57 (2002) 2211.
[11] K. Domelevo, J.-M. Roquejoffre, Existence and stability of travelling wave solutions in a kinetic model of two-phase flows, Commun. Part. Differ. Equ. 24 (1–2) (1999) 61–108.
[12] J.K. Dukowicz, A particle-fluid numerical model for liquid sprays, J. Comput. Phys. 35 (2) (1980) 229–253.
[13] T. Elperin, N. Kleeorin, I. Rogachevskii, D. Sokoloff, Turbulent transport of atmospheric aerosols and formation of large-scale structure, Phys. Chem. Earth A25 (2000) 797–803.
[14] B. Engquist, A.-K. Tornberg, R. Tsai, Discretization of dirac delta functions in level set methods, J. Comput. Phys. 207 (1) (2005) 28–51.
[15] R. Fan, D.L. Marchisio, R.O. Fox, Application of the direct quadrature method of moments to polydisperse gas-solid fluidized beds, Powder Technol. 139 (2004) 7.
[16] R.O. Fox, Computational Models for Turbulent Reacting Flows, Cambridge University Press, Cambridge, 2003.
[17] R.O. Fox, Bivariate direct quadrature method of moments for coagulation and sintering of particle populations, J. Aerosol Sci. 37 (2006) 1562.
[18] R.O. Fox, F. Laurent, M. Massot, Numerical simulation of spray coalescence in an Eulerian framework: direct quadrature method of moments and multi-fluid method, J. Comput. Phys. 227 (6) (2008) 3058–3088.
[19] M. Golomboka, D.B. Pyea, Droplet dynamics in a diesel injection spray, Fuel 69 (9) (1990) 1200–1202.
[20] T. Goudon, F. Poupaud, On the modeling of the transport of particles in turbulent flows, M2AN Math. Model Numer. Anal. 38 (2004) 673–690.
[21] A. Harten, On a class of high resolution total-variation-stable finite-difference schemes, SIAM J. Numer. Anal. 49 (1984) 357–393.
[22] A. Harten, B. Engquist, S. Osher, Chakravarthy, Uniformly high order accurate essentially nonoscillatory schemes, iii, J. Comput. Phys. 71 (1987) 231.
[23] H.M. Hulburt, S. Katz, Some problems in particle technology, Chem. Eng. Sci. 19 (1964) 555.
[24] S. Jin, H. Liu, S. Osher, R. Tsai, Computing multi-valued physical observables for the high frequency limit of symmetric hyperbolic systems, J. Comput. Phys. 210 (2) (2005) 497–518.
[25] S. Jin, H. Liu, S. Osher, Y.-H.R. Tsai, Computing multivalued physical observables for the semiclassical limit of the Schrödinger equation, J. Comput. Phys. 205 (1) (2005) 222–241.
[26] F. Laurent, M. Massot, Multi-fluid modeling of laminar polydisperse spray flames: origin, assumptions and comparison of sectional and sampling methods, Combust. Theor. Model. 15 (5) (2001) 537–542.
[27] H. Liu, S. Osher, Y.-H.R. Tsai, Multi-valued solution and level set methods in computational high frequency wave propagation, Commun. Comput. Phys. 1 (5) (2006) 765–804.
[28] H. Liu, Z. Wang, Superposition of multi-valued solutions in high frequency wave dynamics, J. Sci. Comput. 35 (2–3) (2008) 192–218.
[29] D.L. Marchisio, R.O. Fox, Solution of population balance equations using the direct quadrature method of moments, J. Aerosol Sci. 36 (2005) 43–73.
[30] R. McGraw, Description of aerosol dynamics by the quadrature method of moments, Aerosol Sci. Technol. 27 (1997) 255.
[31] S. Osher, J.A. Sethian, Fronts propagating with curvature-dependent speed: algorithms based on Hamilton-Jacobi formulations, J. Comput. Phys. 79 (1) (1988) 12–49.
[32] L. Sainsaulieu, Equilibrium velocity distribution functions for a kinetic model of two-phase flows, Math. Models Meth. Appl. Sci. 5 (2) (1995) 191–211.
[33] L. Schiller, A. Nauman, A drag coefficient correlation, V.D.I. Zeitung 77 (1935) 318–320.
[34] C.-W. Shu, S. Osher, Efficient implementation of essentially nonoscillatory shock-capturing schemes, J. Comput. Phys. 77 (2) (1988) 439–471.
[35] C.-W. Shu, S. Osher, Efficient implementation of essentially nonoscillatory shock-capturing schemes. II, J. Comput. Phys. 83 (1) (1989) 32–78.
[36] F.A. Williams, Combustion theory, Benjamin Cummings Publ., 1985.